Phases of the Au(100) Surface Reconstruction

Xiao-Qian Wang
Theoretical Physics Institute, University of Minnesota, 116 Church Street S.E., Minneapolis, Minnesota 55455
(Received 28 June 1991)

The temperature-dependent phase behavior of the reconstructed Au(100) surface is studied using molecular-dynamics simulation based on a well tested many-body force scheme. We present the first theoretical description of the three distinct surface structural phases identified by recent x-ray-scattering measurements. Our calculation predicts critical temperatures of the rotational and surface-disordering transitions in good agreement with experimental results, and sheds light on the nature of these phases.

PACS numbers: 68.35.Rh, 64.70.Dv, 68.35.Bs, 68.35.Ja

The reconstruction on the (100) surfaces of noble metals Ir, Pt, and Au has been the subject of much attention. A common feature of this type of reconstruction is a dominant (1×5) pattern with six surface atoms on top of five substrate ones along the $[01\bar{1}]$ direction (henceforth direction y). The Au(100) surface reconstruction, however, exhibits more complicated incommensurate structure which is often referred to as (28×5) or $c(26\times68)$ [1-4]. At room temperature, the orientation of the reconstructed Au(100) hexagonal surface structures can be discontinuously rotated with respect to the underlying square lattice, a feature also observed in Pt(100), but not present in Ir(100). In a recent x-ray-scattering study of Au(100), Mochrie *et al.* [1] identified and characterized three distinct phases between room temperature and the bulk melting transition at $T_M=1337$ K. In the low-temperature phase ($300<T<970$ K), the surface consists of rotated, distorted-hexagonal domains with a fixed rotation angle equal to 0.81° away from the [011] direction (henceforth direction x). At $T_0\simeq970$ K, there is a phase transition to an unrotated hexagonal structure, characterized by the absence of rotated domains. Upon heating, the features associated with the hexagonal order gradually disappear for $T>T_C\simeq1170$ K, leading to an instantaneously disordered, nominally (1×1) high-temperature structure where the square symmetry is recovered.

In spite of this intriguing picture, theoretical studies of these phase transitions are still lacking. It seems important to understand the details of this phase behavior which may serve as a prototype for the study of orientational epitaxy, commensurate-incommensurate reconstructions, order-disorder transitions, and surface melting. In this paper, we directly address these points using a molecular-dynamics (MD) simulation. The main observation of this work is that the formation of rotated domains can be described by a well tested many-body force scheme [5]. In the simulation study with use of the many-body "glue model" parametrized by Ercolessi, Tosatti, and Parrinello [5], the rotated hexagonal order and the overall top-layer hexagonal order decrease abruptly at 950 and 1050 K, respectively, in close agreement with the observed critical temperatures of the rotational and surface-disordering transitions. Our results present a direct confirmation of the experimental characterization for the reconstruction phases, and yield information about the effect of the many-body cohesive forces on these thermodynamic phases.

In carrying out our analysis, we have used a semiempirical many-body force scheme called "glue model" [5] or "embedded-atom method" [6]. This potential is capable of reproducing many features due in reality to the electronic cohesion associated with the d electrons, and allows us to study most metal surfaces for which first-principles calculations are not yet feasible [7]. The Au(100) surface reconstruction, in particular, was explained in considerable detail as arising from the necessity of surface atoms to switch from a poorly packed (100) layer to a (111)-like densely packed configuration [5,7,8]. Previous glue-model studies by Ercolessi, Tosatti, and Parrinello [5] have predicted a bulk melting temperature of $T_M\simeq1350$ K, and a (34×5) geometry for the Au(100) surface reconstruction. However, it remained unclear whether the rotational and surface-disordering transitions could be accounted for by this many-body scheme. Motivated by the experimental findings, we have performed extensive MD simulations, with in-plane periodic boundary conditions, on systems ranging from 2×10^3 to 8×10^3 atoms. The most extensive runs were carried out on an eight-layer slab consisting of 2376 particles as described in Fig. 1. At each temperature, the systems were equilibrated for 2×10^3 time steps (one time step $\simeq7.14\times10^{-15}$ s), and statistics gathered over $(2-7)\times10^3$ time steps. The overall computer experiment consisted of nearly 5×10^5 time steps. Through the simulation study, we have obtained ample results which are concisely described below.

(1) Structure and phases.—A lateral picture of the optimized $T=0$ structure is presented in Fig. 1(a). To obtain the optimized structure, we have performed simulated annealing on $(M\times5)$ reconstruction configurations (i.e., $M+1$ first-layer atoms on top of M second-layer atoms along x, in addition to the 6-onto-5 registry along y), for the range $20<M<36$. Global structure optimization is a very difficult problem for such a large system. The effectiveness of the algorithm depends on the anneal-

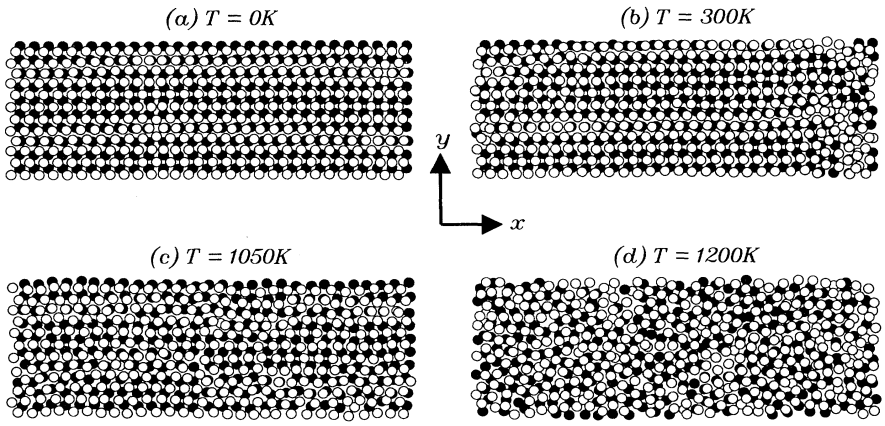

FIG. 1. Top view of the equilibrium structures for the reconstructed Au(100) surface at various temperatures: (a) $T=0$ K, (b) $T=300$ K, (c) $T=1050$ K, and (d) $T=1200$ K. Two (28×5) unit cells are shown. Open and solid circles represent atoms on the top and second layers, respectively. The z direction is along [100] (surface normal), the x direction along [011], and the y direction along $[01\bar{1}]$.

ing procedure and the starting configuration. Various initial atom arrangements, including rotated surface domains, were used to effectively locate the true energy minimum. The structure shown in Fig. 1(a) exhibits a dense hexagonal surface layer on top of a distorted square substrate. The unit cell is regarded as (28×5), where the overlayer contractions are 3.45% along x, and 3.77% along y. The corresponding surface energy is $\sigma=102.0$ meV/Å^2, which is lower than that of 128.5 meV/Å^2 for an unreconstructed (100) surface. The structure is very similar to the (34×5) configuration obtained in the previous studies [5]. The strain along x is concentrated in highly corrugated regions with a one-dimensional "soliton" appearance. Away from the soliton regions, the local surface structure is almost the same as a (1×5) commensurate geometry (*ABCCBA* geometry reported in Ref. [5]). However, the resulting structure is less regular compared with the previously obtained (34×5) configuration: The solitons appear to pull atoms not only along x, but also along y. As an effect of a more careful annealing procedure, the rows are not straight, but exhibit a small modulation. It is worth mentioning that configurations between (26×5) and (38×5) are about equally good in surface energy, as was observed by Ercolessi, Tosatti, and Parrinello [5]. On the other hand, the surface energy difference between the (28×5) and (1×5) configurations is also small, about 0.4 meV/Å^2, providing a rough estimate for the soliton-related strain energy, $\sim$5–10 meV.

The slab was thoroughly equilibrated by MD at $T=300$ K. Depending on the heating rate, our simulation yields two possible configurations. Upon heating slowly, the resulting structure is very similar to that at $T=0$, characterized as aligned domains. Another configuration, which is far more interesting, can be obtained by directly elevating the temperature to 300 K. The distinct feature of this configuration, as is observable in Fig. 1(b), is the overall rotation ($\sim0.7°$) of the surface layer, reminiscent of the experimentally observed rotated domains. A detailed comparison of the aligned and rotated configurations reveals that the compressive strain stress associated with the soliton can be relieved by thermal excitations. Accordingly, the system evolves by a change in the corrugated soliton region and by the formation of domains having new orientations.

Starting from the aligned or rotated configurations, we have studied their structural behavior at elevated temperatures. Figures 1(c) and 1(d) show the structure for the aligned domain, at $T=1050$ and 1200 K, respectively. It is evident that the long-range hexagonal order is well preserved at $T=1050$ K, while it vanishes at $T=1200$ K.

In order to quantify the structural properties, we have computed the static surface structure factor

$$S_Q(\theta)=\frac{1}{N^2}\left\langle\left|\sum_j \exp[i\mathbf{q}(\theta)\cdot\mathbf{R}_j]\right|^2\right\rangle,$$

where the summation is over N surface atoms, $\mathbf{R}_j$ is the position of atom j, $\mathbf{q}(\theta)$ is the wave vector rotated by θ in the vicinity of Q for the hexagonal symmetry, and angular brackets indicate an average over time evolutions. The structure factor has the same symmetry and temperature dependence as the experimentally measured diffraction pattern, characterizing the phases and the hexagonal ordering of the surface.

The structure factor evaluated at various temperatures as a function of rotation angle θ is plotted in Fig. 2 for the aligned (solid curves) and rotated (dashed curves) domains, respectively. The transition to the aligned phase is indicated by the disappearance of peaks associated with the rotated domains [1], and the transition to the disordered phase is characterized by the absence of the central peak for S_Q [1].

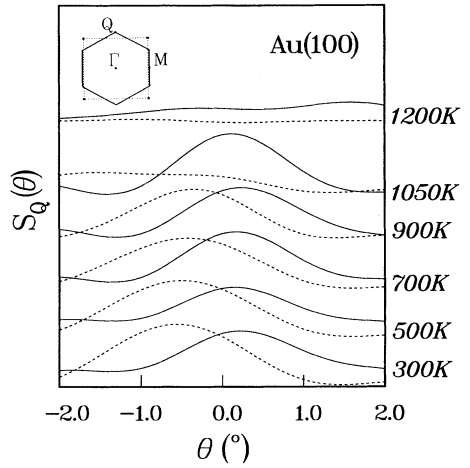

FIG. 2. Calculated surface structure factor as a function of rotation angle θ. Dashed curves represent the results for rotated configurations, and solid curves for the unrotated configurations. Inset: Surface Brillouin zone for hexagonal phases (solid hexagon) and disordered phase (dashed square). Hexagonal reciprocal-lattice vectors Γ, Q, and M are indicated by solid circles.

(2) The rotational transition.—The rotation angle of the reconstructed domains is characterized by the peak position of S_Q. Figure 3 displays the rotation angle θ^* and the corresponding static surface structure factor $S_Q(\theta^*)$ for rotated domains. At room temperature, the rotation angle is 0.65°, in good agreement with experimental values of 0.81° by x-ray scattering [1] and of 0.5°–0.7° by transmission electron microscope study [2]. The rotation angle has a weak temperature dependence, slightly decreasing to 0.4° at 950 K, in qualitative agreement with experimental observations [1]. Above 950 K, $S_Q(\theta^*)$ drops drastically as the temperature increases. The picture that emerges from Figs. 2 and 3 is that below T_0, the rotated domains coexist with the aligned ones. This has been confirmed by studies of configurations with larger sizes (not shown). Above T_0, the aligned domain dominates the structural feature.

(3) Surface-disordering transition.—In Fig. 4 we present a plot of the in-plane average-main-square (rms) displacement σ_n for the top three layers and the static structure factor, as a function of temperature. It is clear that the structure factor and σ_n remain almost constant at $T=1050$ K and below, while above 1050 K, the static surface structure factor drops abruptly, accompanied by the sharp increase of the first-layer rms displacement, indicating a phase transition. The transition temperature T_C can be estimated from Fig. 3: $T_C \simeq 1050$ K, in reasonably good agreement with the experimental value of 1170 K by Mochrie and co-workers [1,4].

Above T_C, the diffusion in the surface layers is liquidlike, in close analogy to the surface melting phenomenon. In fact, the disordered (1×1) phase may be regarded as

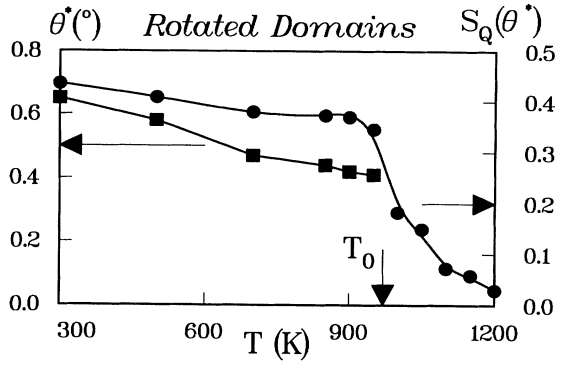

FIG. 3. The rotation angle θ^* (circles) and the corresponding static structure factor $S_Q(\theta^*)$ (squares) as a function of temperature for rotated domains. The theoretical critical temperature for the rotational transition is $\simeq 950$ K, in good agreement with the experimental value of $T_0=970$ K.

the consequence of a particular melting process, where, in contrast to conventional melting, the quasiliquid thickness does not increase rapidly as the temperature is raised towards T_M. Owing to the residual order induced by the substrate, (1×1) features can be observed in a diffraction pattern. It is worth mentioning that the similar behavior of "blocked surface melting" has been observed in gold clusters [9], and it is worth noting that in connection with the strong electronic cohesion, surfaces of gold exhibit strikingly different surface-melting behavior compared with that of Lennard-Jones surfaces [10].

In summary, we have reported new theoretical results on the reconstructed Au(100) surface, using the glue model and MD simulation. The results, obtained without introducing adjustable surface parameters, reveal the rotational and surface-disordering transitions, and suggest that the surface strain described by the many-body force

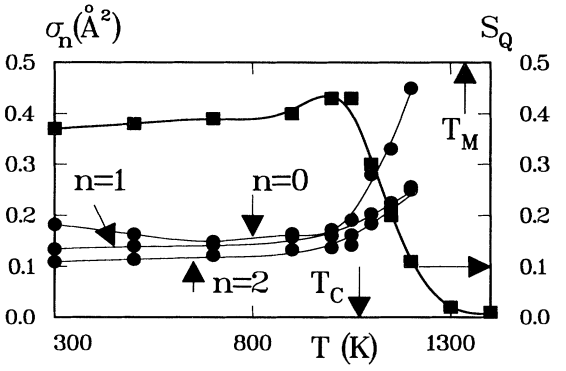

FIG. 4. The rms in-plane vibrational amplitude (circles) for the nth layer (σ_n) and the static surface structure factor at Q (squares) as a function of temperature. The surface layer corresponds to $n=0$. The estimated critical temperature for the surface-disordering transition is $\simeq 1050$ K, in reasonably good agreement with the experimental value of $T_C=1170$ K.

scheme, which is responsible for driving surface reconstruction [5,8], is also relevant to the formation of rotated domains. It is gratifying that the many-body force scheme can provide a consistent description of the phase behavior for the Au(100) surface reconstruction, and the simulation results should have an impact on studies of similar phenomena on other surfaces, notably on Au(111) [11] and Si(100) [12].

X-Q.W. would like to thank C. E. Campbell, F. Ercolessi, E. Tosatti, and C. Z. Wang for stimulating discussions. This work is supported in part by the Minnesota Supercomputer Institute through a Research Scholarship and a Cray-2 grant.

[1] S. G. J. Mochrie, D. M. Zehner, B. M. Ocko, and Doon Gibbs, Phys. Rev. Lett. **64**, 2925 (1990); Doon Gibbs, B. M. Ocko, D. M. Zehner, and S. G. J. Mochrie, Phys. Rev. B **42**, 7330 (1990); B. M. Ocko, D. Gibbs, K. G. Huang, D. M. Zehner, and S. G. J. Mochrie, Phys. Rev. B **44**, 6429 (1991).

[2] K. Yamazaki, K. Takayanagi, Y. Tanishiro, and K. Yagi, Surf. Sci. **199**, 595 (1988).

[3] G. Binnig, H. Rohrer, Ch. Gerber, and E. Stoll, Surf. Sci. **144**, 321 (1984).

[4] D. Gibbs, B. M. Ocko, D. M. Zehner, and S. G. J. Mochrie, Phys. Rev. B **38**, 7303 (1988).

[5] F. Ercolessi, E. Tosatti, and M. Parrinello, Phys. Rev. Lett. **57**, 719 (1986); Surf. Sci. **177**, 314 (1986).

[6] M. S. Daw and M. I. Baskes, Phys. Rev. B **29**, 6443 (1984).

[7] N. Takeuchi, C. T. Chan, and K. M. Ho, Phys. Rev. Lett. **63**, 1273 (1989); Phys. Rev. B **43**, 14363 (1991).

[8] B. W. Dodson, Phys. Rev. Lett. **60**, 2288 (1988).

[9] A. Bartolini, F. Ercolessi, and E. Tosatti, Phys. Rev. Lett. **63**, 872 (1989); F. Ercolessi, W. Andreoni, and E. Tosatti, *ibid.* **66**, 911 (1991).

[10] P. Carnevali, F. Ercolessi, and E. Tosatti, Phys. Rev. B **36**, 6701 (1987).

[11] K. G. Huang, D. Gibbs, D. M. Zehner, A. R. Sandy, and S. G. J. Mochrie, Phys. Rev. Lett. **65**, 3313 (1990).

[12] O. L. Alerhand, D. Vanderbilt, R. D. Meade, and J. D. Joannopoulos, Phys. Rev. Lett. **61**, 1973 (1988), and references therein.